

## Research Paper

# Optimization of Drilling Parameters for Aluminum Metal Matrix Composite Using Entropy-Weighted TOPSIS under MQL Conditions

Sachin G. GHALME<sup>1</sup>, Paweł KAROLCZAK<sup>2</sup>\*

<sup>1</sup> *Department of Mechanical Engineering  
Sandip Institute of Technology and Research Centre  
Nashik (MS), India; e-mail: e-mail:sachin.ghalme@sitrc.org*

<sup>2</sup> *Wroclaw University of Science and Technology  
Faculty of Mechanical Engineering  
Wroclaw, Poland*

\*Corresponding Author e-mail: pawel.karolczak@pwr.edu.pl

The aim of the present work is to understand the effect of drilling parameters (drill speed and feed rate) during the drilling of a Saffil fiber-reinforced Al metal matrix composite (MMC) under minimum quantity lubrication (MQL) condition. The effect of drilling parameters on individual response characteristics is evaluated and the optimum drilling parameters are also investigated using a multi-response optimization technique known as the entropy-weighted technique for order performance by similarity to ideal solution (EWTOPSIS). The drilling parameter optimization is performed with the aim of minimizing surface roughness in the drilled hole, roundness error in the drilled hole and feed force during drilling. The drilling parameters have a significant effect on individual responses. Weights were assigned to each response using the entropy weight method, and closeness coefficients were calculated to obtain the optimal level for the drilling parameters. A drill speed of 11 m/min and a feed rate of 0.05 mm/rev are the optimal combination to minimize the desired output responses simultaneously.

**Keywords:** Al metal matrix composite; drilling; parameter optimization; entropy weight; Grey relational analysis.

## 1. INTRODUCTION

Modern construction materials used in the construction of machines, and especially in means of transport, must exhibit improved properties, particularly strength, when compared to other materials. The breakthroughs came with the development of metal matrix composites (MMCs) with continuous fibres and whiskers as reinforcement. They were developed in the 1970s [1]. Compos-

ite materials consist of at least two materials with clearly defined boundaries, forming them through the sharing of the total volume. When integrated, they form a material with properties different from those of an individual component. Composite materials are heterogeneous on a microscopic scale, but homogeneous on a macroscopic scale. They consist of the so-called matrix and reinforcement. Compared to matrix metals, composites offer many advantages, such as higher specific strength, higher temperature resistance, lower thermal expansion coefficient, and better wear resistance. These properties make composites ideal for applications in the automotive, aviation, space, and electronic industries [2]. Among metal composites, the most commonly used are those have aluminium alloys as a matrix. Aluminum matrix composites (AMC) have found applications in a variety of engineering applications and are well known for their strength-to-weight ratio. In addition, AMCs are characterized by good stiffness, high corrosion resistance, a high specific modulus, and excellent wear resistance properties [3].

The most common methods for producing ceramic-reinforced aluminum composites are casting, powder metallurgy, and spray deposition [4, 5]. However, often additional manufacturing techniques are necessary in the production cycle to obtain the required dimensional tolerance and appropriate surface finish. Machining offers such possibilities. The biggest challenge in machining of aluminum composites is the abrasive nature of the reinforcement. This is a serious risk to cutting tools. Tools wear more rapidly when machining aluminum composites compared to aluminum alloys [6, 7]. Therefore, it is recommended to use tools made from sintered carbides and polycrystalline diamond [8]. Various manufacturing techniques are used to make a hole in a composite. For holes with a small diameter of up to 1 mm, laser drilling is considered the ideal method [9]. Electrical discharge machining (EDM) may be a method for minimizing blade wear [10]. However, in the case of nearly all types of composites, drilling remains the most frequently performed operation to make a hole [11].

Much work has been conducted to investigate the impact of drilling process input parameters and cutting tools on the final MMC components. For the SiCp/Al drilling, HUANG *et al.* [12] emphasized that variations in the feed rate play a key role in determining drilling performance. Similarly, RAJMOHAN *et al.* [13] also found that the feed rate is the main parameter influencing the machining rather than the drilling speed in SiC/Al356 hybrid composites. With regard to tool life, it has been observed that drilling speed has a minimal effect, while the tool life is significantly reduced due to variations in the feed rate. Additionally, tool service life mainly depends on the hardness of the reinforcement, the chemical composition of the matrix, and the reinforcement material for the drilling operation. The quality of MMC drilled surfaces depends on the material of the drilling tool, the matrix material, feed rate and cutting speed [14].

Composites are materials difficult to machine. The effect of reinforcement has a significant impact not only on the cutting tool's life, but also on cutting forces and the quality of the finished products. Therefore, a lot of research is being conducted on the optimization of machining parameters to obtain the best technological results. In this work, our aim is to obtain the optimal level of drilling speed and feed rate to minimize surface roughness of drilled hole, roundness error in the drilled hole, and feed force during the drilling operation. This becomes a case of multi-criteria decision making (MCDM) or multi-response optimization, where we attempt to optimize input variables for multiple response variables simultaneously. Various methods are available for multi-response optimization, including the multi-response signal-to-noise ratio method (MRSN), weighted signal-to-noise ratio method (WSN), grey relational analysis (GRA), principal component analysis (PCA), and technique for order preference by similarity to ideal solution methods (TOPSIS), among others.

BUTOLA *et al.* [15] investigated hybrid aluminum composites reinforced with sugar cane ash, peanut shells, and jute. The weight proportions of the reinforcement were 3 wt%, 6 wt%, and 9 wt%. These materials were turned, and optimization was performed using genetic algorithm (GA) and response surface methodology (RSM) methods. It was found that for composites with 3% and 9% reinforcement, the depth of cut had the greatest impact on achieving minimum roughness. The optimal value of the input parameters given by RSM was 1000 rpm, a feed rate of 0.15 mm/rev, and a depth of cut of 0.3 mm for all three composites. SENTHILKUMAR [16] optimized electric discharge machining (EDM) parameters for machining aluminum alloy to obtain the minimum surface roughness and maximum layer thickness using TOPSIS. The surface roughness and layer thickness obtained through TOPSIS were 4.55  $\mu\text{m}$  and 112.08  $\mu\text{m}$ , respectively, with the optimal level of 10 amps for current, a 500  $\mu\text{s}$  pulse on time, and a 500  $\mu\text{s}$  pulse off time.

The turning of ceramic-reinforced aluminum was optimized by RAMAKRISHNAN *et al.* [17]. The ANNOVA method was employed to calculate cutting regression models, and the TOPSIS method to calculate the optimal parameters. The maximum material removal rate (MRR) (6.021  $\text{cm}^3/\text{min}$ ) was obtained at the maximum values of speed (1750 rpm), feed (1.5 mm) and cutting depth (0.8 mm). The feed had the most substantial influence on attaining the maximum MRR, followed by the depth of cut. Conversely, the minimum surface roughness (0.26  $\mu\text{m}$ ) was achieved with the minimum values of speed, feed, and depth of cut. In this case, the feed had the greatest impact on achieving minimum roughness.

REDDY *et al.* [18] investigated the drilling process of a TiC-reinforced aluminum composite. The volume content of the reinforcement was 10%. The ANOVA GRG analysis showed that the helix angle of the drill bit had the great-

est impact on the technological effects (63.2%), followed by the feed with a share of 34%. The speed at 2.7% had the smallest contribution to the optimization of the drilling parameters when drilling this material. The optimal drilling parameters identified by the GRA method were as follows: the largest used helix angle ( $40^\circ$ ), the average spindle speed (500 rpm) and the lowest feed rate (0.1 mm/rev). ABBAS *et al.* [19] investigated the high speed drilling process for Al/SiC metal matrix composite. They analyzed thrust force, hole diameter, delamination factor, surface roughness, tool wear and chips analysis at different spindle speeds (3000–9000 rpm) and feed rates (0.05–0.2 mm/rev). They found that moderate drilling speeds between 5000 and 7000 rpm are suitable for drilling Al/SiC metal matrix composite in terms of all parameters.

The growing interest in composite materials makes it very important to understand their machinability. The substantial differences in properties between the matrix and reinforcement make these materials difficult to machine. In addition, the vast variety of these materials means that continuous research is needed on their machinability and the optimization of input parameters in the machining process to obtain the highest-quality results of machining. Despite improvements in machining techniques, dry machining alone is not sufficient for all industrial needs. It is also evident that cooling and lubrication also have significant effect in the drilling process of composites. In most cases, immersion lubrication is employed during machining, but this increases cost of manufacturing and pose problems related waste disposal. To overcome these issues, innovative methods of cooling and lubrication, such as cryogenic cooling and minimum quantity lubrication (MQL) are used, showing good results in terms of machining response. However, it should be noted that the use of MQL can generate oil mist through compressed air mixed lubricating oil, which is hazardous to operators. Since the early 2000s, the MQL has been considered a sustainable alternative to flood lubrication. It is also known as near-dry machining, as it consumes 10 000 times less fluid volume when mixed with air, thereby reducing fluid consumption [20].

In one of the earliest study on MQL, VARADARAJAN *et al.* [21] evaluated dry machining, flood cooling and MQL during hard turning AISI 4340 steel. During machining, MQL was found to be efficient in reducing surface roughness, cutting force, cutting temperature and chip-tool contact length, leading to an extended tool life. KANNAN *et al.* [22] studied the machinability of an aluminum matrix nanocomposite under dry and MQL conditions. Machining under MQL condition reduced tool wear and cutting force due to the lubricating effect of oil mist, thereby reducing friction and heat. The high fluid pressure also contributed to effective chip breaking, thereby improving surface roughness. Numerous articles have presented the effectiveness and benefits of MQL during machining [23, 24].

The subject of the present research is an aluminum metal matrix composite material. The matrix of the tested material is a multi-component aluminum casting alloy with the designation AlSi9Mg, and the reinforcement is made of ceramic fibers called Saffil. The impact of machining parameters under the influence of MQL is investigated in this work. In this study, we employ the entropy-weighted TOPSIS methodology to obtain the optimal level of drilling speed and feed rate for minimizing surface roughness of the drilled hole, roundness error in the drilled hole, and feed force during the drilling operation. The effect of drilling parameters on individual responses with MQL lubrication is also investigated. Despite extensive research on the machinability of MMCs, further work on this topic is needed. This arises from the wide variety of composite materials, which differ in matrix material, reinforcement, reinforcement shape, arrangement, and volumetric content of the reinforcement, making it difficult to compare published research results and relate them to a specific newly designed composite material. The test results presented broaden the understanding of the machinability of aluminum composite materials. They are also part of the research conducted at Wroclaw University of Science and Technology on increasing the efficiency of manufacturing elements from these materials.

## 2. MATERIALS AND METHODS

### 2.1. Materials

An aluminum alloy EN AC-43330 (AlSi9Mg) cast aluminum is used as matrix for the composite preparation. The chemical composition and properties of aluminum alloy EN AC-43330 (AlSi9Mg) are presented in Tables 1 and 2, respectively.

**Table 1.** Chemical composition of aluminum alloy EN AC-43330 (AlSi9Mg).

Al	Si	Cu	Mg	Mn	Fe	Ti	Zn
rest	9.5	<0.05	0.35	<0.1	<0.18	0.15	0.07

**Table 2.** Properties of aluminum alloy EN AC-43330 (AlSi9Mg).

Density [g/cm <sup>3</sup> ]	Tensile strength: yield [MPa]	Tensile strength: ultimate [MPa]	Young's modulus [GPa]	Brinell hardness
2.5	210–230	280–290	71	91–94

The strength of the composite material is determined by the reinforcement. Saffil fibers used in the tested material are one of the most frequently used materials for the reinforcement of metal matrix composite. Saffil ceramic fibers are used as the reinforcement in the aluminum metal matrix. They belong to a group

of high-strength materials, as they are characterized by good resistance to high temperatures, high tensile strength and a high modulus of elasticity [25]. The chemical composition and properties are presented in Tables 3 and 4, respectively.

**Table 3.** Chemical composition of Saffil fiber.

Al <sub>2</sub> O <sub>3</sub>	SiO <sub>2</sub>	Fe, Cr, Ni, Na, Mg, Ca, chlorides
96–97%	3–4%	Trace amounts

**Table 4.** Properties of Saffil fiber [26].

Density [gm/cm <sup>3</sup> ]	Tensile strength [MPa]	Compressive strength [GPa]	Young's modulus [GPa]	Rupture modulus [GPa]	Durable up to temperature [°C]
3.3–3.5	1200–1800	14 700–26 700	300–330	300–340	1600

## 2.2. Fabrication of composite

The MMC composites are produced using a squeeze casting process. In squeeze casting, applied pressure improves the bonding between Al alloy matrix and Saffil fiber. In this process, 10 vol% of Saffil fiber is added to the aluminum metal matrix. A Saffil fiber block is created by mixing Saffil fibers with a silica binder, pouring the mixture into a mould, filtering off the solution, drying the profile with hot air and firing it at a temperature of 950°C. Figure 1 shows initial image of Saffil fiber with created Saffil fiber block and Fig. 2 shows the SEM image for Saffil fiber.

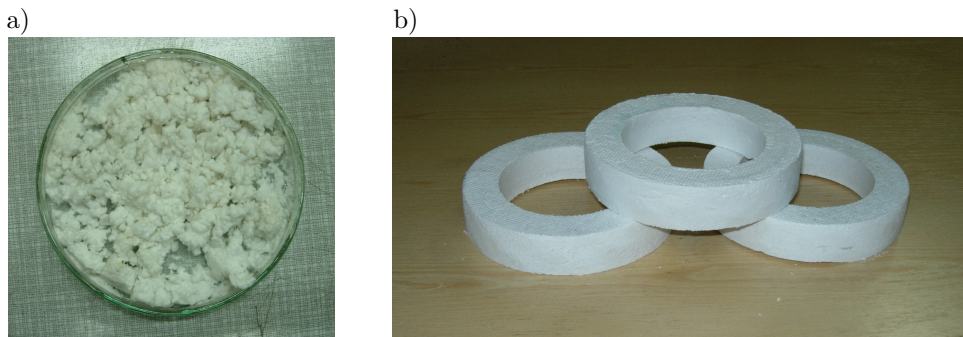


FIG. 1. Saffil fiber (a), and Saffil fiber block (b).

The block heated to 700°C is placed in a mould, and liquid aluminium is poured over it. Pressure is exerted to the surface of the metal by means of a ram.

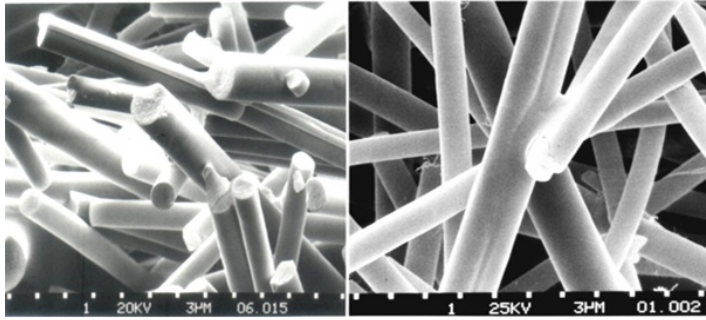


FIG. 2. SEM image for Saffil fiber.

The ram and the mould containing the block are heated to the temperature of 150–300°C [27]. Due to the properties of the reinforcement fibers, compared to the matrix, the tested composite is characterized by an increase in hardness (by 50%) and tensile strength (by 60%). The yield point also increases (by 40%). Figure 3 shows metallographic polished section of the tested Al MMC sample. It shows evenly distributed Saffil fibers in the aluminum matrix.

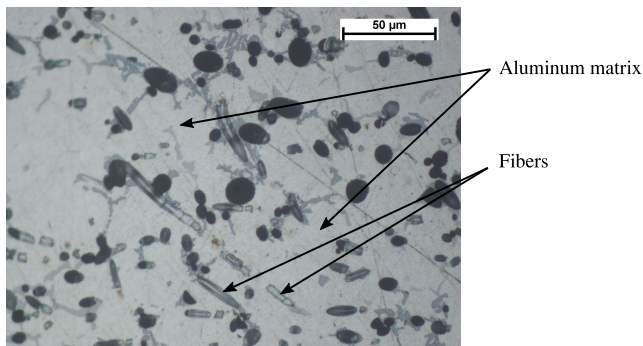


FIG. 3. Metallographic polished section of the tested composite.

### 2.3. Drilling of composite

Drilling tests were carried out on a Csepel RF 50/1250 radial drilling machine. The MMC samples were in the form of blocks with a 120 mm diameter. A carbide drill with the designation 6537 VHM TiAlN and a diameter of 9.9 mm was used to for drilling. A fresh tool was used for each drilling condition (allowing for two holes). TiAlN was used as the coating for the sintered carbides, which is characterized by good adhesion, high strength, and abrasion resistance. The machine was equipped with an attachment of Accu-Lube Mini booster for MQL. The cooling lubricant in the form of aerosol was fed with the help of nozzle near the drill bit. An oil mist of Lb5000 lubricating oil was generated

at an operating pressure of 7 bar and an oil flow rate of 180 ml/hr. Table 5 shows properties of lubricating oil used. Each test was performed twice, and results were recorded to minimize the error. A brief summary of experimental conditions is shown in Table 6, and the experimental setup is depicted in Fig. 4.

**Table 5.** Properties of Lb5000 oil.

Lb5000 Oil	Density [kg/m <sup>3</sup> ]	Solidification temperature [°C]	Flash point [°C]	Stickiness in 40°C	Solubility in water
	850	50	190	18	No

**Table 6.** Summary of experimental conditions.

Machine	Csepel RF 50/1250 radial drilling machine
Drill type	Carbide drill, 6537 VHM TiAlN, diameter: 9.9 mm
Work piece	Saffil/Al metal matrix composite
Drill speed [m/min]	11, 22, 44
Feed rate [mm/rev]	0.05, 0.075, 0.112, 0.17

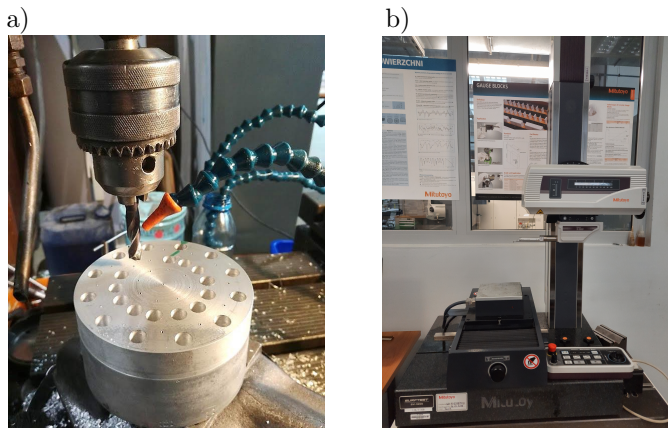


**FIG. 4.** Drilling setup with oil mist feeding arrangement (a), and measurement of surface roughness with Mitutoyo Surftest SV-3200 (b).

The quality of the drilled holes was assessed by measuring errors in shape (roundness) and surface roughness. Roundness for the drilled hole was measured with a Taylor-Hobson device of the Talyrond 265 type. The drilled hole's surface roughness was measured with the Mitutoyo Surftest SV-3200 roughness tester. The 2D roughness measurements were carried out along a measuring length of 4.8 mm. The surface roughness was measured at four different locations and the average results were used for analysis.

During the drilling process, the feed force and the cutting torque were measured. A measuring circuit was used for this purpose, which consisted of a piezo-electric dynamometer type 9257A from KISTLER, an electric signal amplifier type 5011 from the same company, and an oscilloscope type TDS 5054B from Tektronix.

### 3. RESULTS AND DISCUSSION

The primary aim of this work was to determine the best value for drill speed and feed rate within the range of tested parameters to minimize surface roughness of the drilled hole, roundness error in the drilled hole and the feed force during the drilling of Saffil fiber-reinforced Al MMC. The experimental run conditions and the average values of responses are presented in Table 7.

**Table 7.** Experimental run conditions and average values of responses results.

Test no.	Drill speed [m/min]	Feed rate [mm/rev]	Surface roughness [ $\mu\text{m}$ ]	Roundness error [ $\mu\text{m}$ ]	Feed force [N]
1	11	0.05	2.2	18.46	194.16
2		0.075	3.17	15.17	251.33
3		0.112	3.32	38.26	334.69
4		0.17	5.82	43.2	456.99
5	22	0.05	3.65	22.04	168.57
6		0.075	3.42	15.56	247.8
7		0.112	3.36	11.69	327.8
8		0.17	5.62	99.27	490.38
9	44	0.05	3.59	42.76	185.73
10		0.075	3.53	23.37	232.41
11		0.112	2.39	20.89	332.59
12		0.17	5.04	73.21	484.9

Based on experimental results, it is difficult to predict the optimal drilling parameters that would simultaneously minimize all responses.

#### 3.1. Effect of drilling parameters on individual response

*3.1.1. Surface roughness.* Figure 5a shows the main effect plot for surface roughness, revealing the impact of individual parameters on surface roughness. In the case of drill speed, the surface roughness value increases for the drill speed in the range from 11 m/min to 22 m/min and next decreases for 44 m/min. In the case of feed rate, the surface roughness value increases for the feed rate range from 0.05 mm/rev to 0.075 mm/rev and then decreases with a subse-

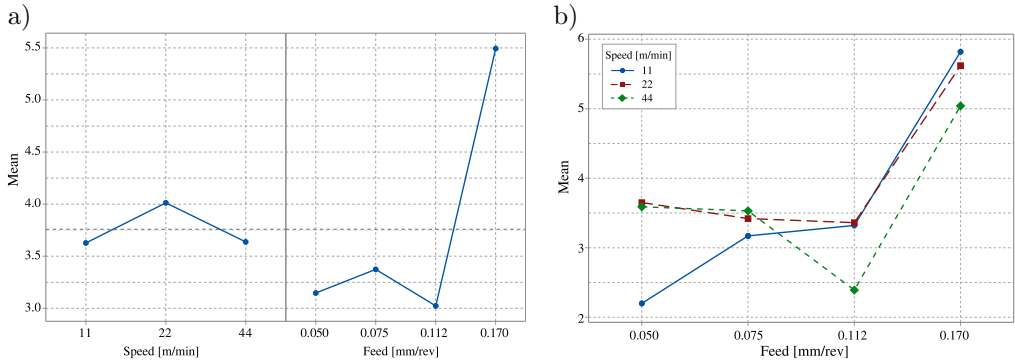


FIG. 5. The main effect plot for surface roughness [μm] (a), the interaction plot for surface roughness [μm] (b).

quent increase for 0.17 mm/rev. Figure 5b shows interactive effect of drilling parameters for surface roughness. Analyzing the interactive effect, it is evident that a drill speed of 11 m/min and a feed rate of 0.05 mm/rev are optimal for achieving the minimum value for surface roughness individually.

3.1.2. Roundness error. Figure 6a shows the main effect plot for roundness error in the drilled hole, showing the effect of individual parameters on roundness error. In the case of speed, the roundness error value increases from 11 m/min to 44 m/min. In the case of feed rate, the roundness error value decreases from 0.05 mm/rev to 0.075 mm/rev and then increases to 0.17 mm/rev. Figure 6b shows the interactive effect of drilling parameters for roundness error in the drilled hole. Analyzing the interactive effect, it is evident that a drill speed of 22 m/min and feed of 0.112 mm/rev are optimal for achieving the minimum value for roundness error individually.

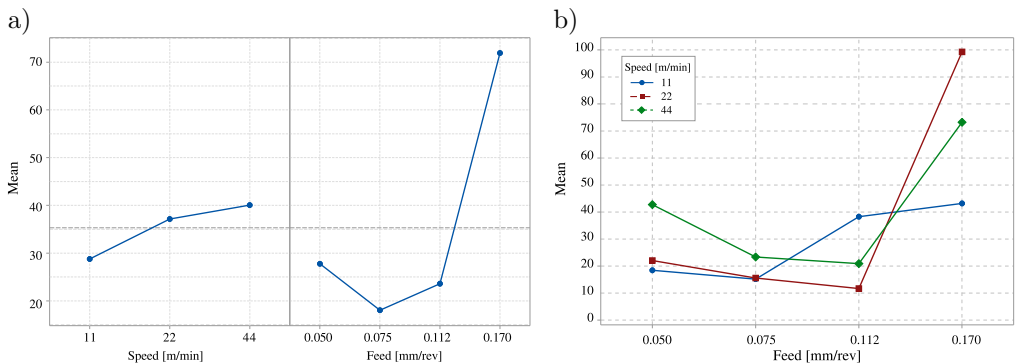


FIG. 6. The main effect plot for roundness error [μm] (a), the interaction plot for roundness error [μm] (b).

*3.1.3. Feed force.* Figure 7a shows the main effect plot for feed force during drilling hole, showing the influence of individual parameters on feed force. It is interesting to note that drill speed does not have a significant effect on feed force. In the case of feed rate, the feed force value increases from 0.05 mm/rev to 0.17 mm/rev. Figure 7b shows the interactive effect of drilling parameters for feed force during drilling hole. Examining the interaction effect, it becomes evident that drill speed and feed have a significant interaction effect on feed force. When analyzing the interactive effect, it is evident that a drill speed of 22 m/min and a feed rate of 0.05 mm/rev are optimal for achieving the minimum value for feed force individually.

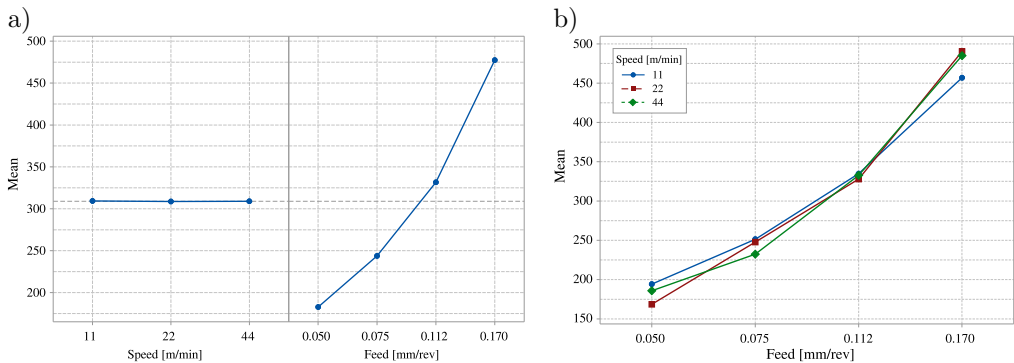


FIG. 7. The main effect plot for feed force [N] (a), the interaction plot for feed force [N] (b).

As seen from the above discussion, individual responses require different combinations of drilling parameters to achieve the minimal value. In order to obtain the best combination of drill speed and feed rate for achieving minimal values for surface roughness, roundness error and feed force the entropy-weighted grey relational analysis (EWGRA) was performed as explained further.

### 3.2. Entropy weight calculation for response variable

In 1948, Shannon proposed the EWM [28], and Zeneley further improved it in 1982. The EWM is an effective method to assign weights to identified criteria or responses in MCDM [29–31]. According to WANG *et al.* [29], the EWM is an objective weighing process based on neutral data and it can overcome the shortcomings of the subjective weighing method. The EWM is a highly successful strategy for calculating weights to assess response indicators. The following steps outline the process of calculating EW [32]:

*Step 1.* Normalization of decision matrix.

Let there be  $n$  response variable with  $m$  values, and the decision matrix is represented as:

$$(3.1) \quad \mathbf{A} = (a_{ij})_{mn} = \begin{bmatrix} a_{11} & \cdots & a_{1n} \\ \vdots & \ddots & \vdots \\ a_{m1} & \cdots & a_{mn} \end{bmatrix}.$$

Since response variables may be with different units, it is necessary to normalize the data within the range of 0 to 1. Equation (3.2) is used to normalize the beneficial response and Eq. (3.3) is used to normalize the non-beneficial response.

$$(3.2) \quad NMa_{ij} = \frac{a_{ij}}{\max a_{ij}},$$

$$(3.3) \quad NMa_{ij} = \frac{\min a_{ij}}{a_{ij}}.$$

In this work, all three responses-surface roughness, roundness error and feed force are undesirable, so Eq. (3.3) is used for normalization. After normalization of the response, the probability of the response is calculated using Eq. (3.4):

$$(3.4) \quad P_{ij} = \frac{a_{ij}}{\sum_{i=1}^m a_{ij}}.$$

*Step 2.* Calculation of entropy for each index.

$$(3.5) \quad E_j = -\frac{1}{\ln m} \sum_{i=1}^m P_{ij} \ln P_{ij}, \quad j = 1, 2, 3, \dots, n.$$

*Step 3.* Calculation of degree of deviation for each response.

$$(3.6) \quad D_j = |1 - E_j|, \quad j = 1, 2, \dots, n,$$

where  $D_j$  measures the degree of deviation of essential information for the  $j$ -th criterion.

*Step 4.* Calculation of entropy weight.

$$(3.7) \quad w_j = \frac{D_j}{\sum_{j=1}^m D_j},$$

where  $w_j$  is the importance weight of the  $j$ -th criterion.

The entropy weight calculation and weights in terms of percentage for each response are shown in Table 8.

**Table 8.** Entropy weight calculation.

Calculation	Surface roughness	Roundness error	Feed force
$\sum_{i=1}^m P_{ij} \ln P_{ij}$	-2.4455	-2.3370	-2.4244
$E_j = -\frac{1}{\ln m} \sum_{i=1}^m P_{ij} \ln P_{ij}$	0.9841	0.9405	0.9456
$D_j =  1 - E_j $	0.0159	0.0595	0.0244
$w_j = \frac{D_j}{\sum_{j=1}^m D_j}$	0.16	0.60	0.24
% Weight	16%	60%	24%

### 3.3. Optimization using TOPSIS method

In the area of multi-criteria decision making, TOPSIS is a simple and appropriate methodology for obtaining a solution in multi-response optimization. TOPSIS was proposed by HWANG and YOON in 1981 [33]. It is based on the principle that the optimal solution has the shortest distance from the positive ideal solution and the maximum distance from the negative ideal solution. In essence, TOPSIS provides a solution that is farthest away from the hypothetical worst and closest to the hypothetical best solution.

Numerous researchers employed TOPSIS for optimization. For example, MANIVANNAN and KUMAR [34] implemented TOPSIS for optimizing cryogenically cooled EDM drilling parameters, while THIRUMALAI and SENTHILKUMAR [35] used NSGA II and TOPSIS for optimizing machining parameters in the turning of Inconel 718. TOPSIS was used for the selection of better alternatives from the non-dominated solutions. SINGH *et al.* [36] used TOPSIS for optimizing discharge current, pulse on duration, and dielectric fluid pressure to improve EDM process performance. The step-wise implementation of the TOPSIS method in the current research work is presented below [37–39]:

*Step 1.* Construction of decision matrix.

In multi-objective problems using TOPSIS, the averaged values of every output response for every experiment are arranged in the form of matrix known as a decision matrix, as per Eq. (3.8):

$$(3.8) \quad \mathbf{D} = \begin{bmatrix} x_{11} & x_{12} & x_{13} & \cdots & \cdots & x_{1n} \\ x_{21} & x_{22} & x_{23} & \cdots & \cdots & x_{2n} \\ x_{31} & x_{32} & x_{33} & \cdots & \cdots & x_{3n} \\ \cdots & \cdots & \cdots & \cdots & \cdots & \cdots \\ \cdots & \cdots & \cdots & \cdots & \cdots & \cdots \\ x_{m1} & x_{m2} & x_{m3} & \cdots & \cdots & x_{mn} \end{bmatrix},$$

where  $n$  represents response variables with  $m$  corresponding alternatives/values.

*Step 2.* Normalization of decision matrix.

Response variables may have different dimensions and scales, requiring conversion into non-dimensional characteristics for mutual comparison across the criteria. The decision matrix is further normalized using Eq. (3.9):

$$(3.9) \quad r_{ij} = \frac{x_{ij}}{\sqrt{\sum_{i=1}^m x_{ij}^2}}, \quad i = 1, 2, \dots, m; \quad j = 1, 2, \dots, n.$$

*Step 3.* Calculation of weighted normalized matrix.

In this step, the normalized response variables are multiplied by respective weights, as obtained from the EWC presented in Subsec. 3.2. The final values of weights are 16% for surface roughness, 60% for roundness error, and 24% for feed force, as presented in Table 8; the weighted normalized matrix is calculated using Eq. (3.10):

$$(3.10) \quad v_{ij} = w_j * r_{ij}, \quad i = 1, 2, \dots, m; \quad j = 1, 2, \dots, n.$$

The values of the normalized matrix and weighted normalized matrix for tensile strength, flexural strength and impact strength are presented in Table 9.

**Table 9.** The values of the normalized and weighted normalized response variables.

Test	Normalized matrix for response variables			Weighted normalized matrix for response variables		
	Surface roughness	Roundness error	Feed force	Surface roughness	Roundness error	Feed force
1	0.328	0.897	3.189	0.052	0.538	0.765
2	0.472	0.737	4.128	0.076	0.442	0.991
3	0.494	1.858	5.497	0.079	1.115	1.319
4	0.867	2.098	7.505	0.139	1.259	1.801
5	0.543	1.071	2.769	0.087	0.642	0.664
6	0.509	0.756	4.070	0.081	0.453	0.977
7	0.500	0.568	5.384	0.080	0.341	1.292
8	0.837	4.822	8.054	0.134	2.893	1.933
9	0.535	2.077	3.050	0.086	1.246	0.732
10	0.526	1.135	3.817	0.084	0.681	0.916
11	0.356	1.015	5.462	0.057	0.609	1.311
12	0.750	3.556	7.964	0.120	2.134	1.911

*Step 4.* Determination of the positive ideal (best) and negative ideal (worst) solutions.

The positive ideal (best) solution enhances the desired response variables and the negative ideal (worst) solution diminishes the desired response variables. The positive ideal and negative ideal solutions are calculated using Eqs. (3.11) and (3.12):

- the positive ideal solution:

$$(3.11) \quad A^+ = \{v_1^+, v_2^+, \dots, v_n^+\} \\ = \{(\max_i v_{ij} | j \in J), (\min_i v_{ij} | j \in J') | 1, \dots, m\},$$

- the negative ideal solution:

$$(3.12) \quad A^- = \{v_1^-, v_2^-, \dots, v_n^-\} \\ = \{(\min_i v_{ij} | j \in J'), (\max_i v_{ij} | j \in J) | 1, \dots, m\},$$

where  $J = \{j = 1, 2, \dots, n | j\}$ : associated with the beneficial response variables,  $J' = \{j = 1, 2, \dots, n | j\}$ : associated with the non-beneficial response variables.

The evaluated values of the positive ideal (best) and negative ideal (worst) solutions are presented in Table 10.

**Table 10.** The values of the positive ideal and negative ideal solutions.

Response variable	Positive ideal solution	Negative ideal solution
Surface roughness	0.052	0.139
Roundness error	0.442	2.893
Feed force	0.664	1.933

*Step 5.* Calculation of distance from ideal solution. The distance of each alternative from the positive ideal solution ( $S_i^+$ ) and from the negative ideal solution ( $S_i^-$ ) are calculated using Eqs. (3.13) and (3.14):

$$(3.13) \quad S_i^+ = \sqrt{\sum_{j=1}^n (v_{ij} - v_j^+)^2}, \quad i = 1, 2, \dots, m,$$

$$(3.14) \quad S_i^- = \sqrt{\sum_{j=1}^n (v_{ij} - v_j^-)^2}, \quad i = 1, 2, \dots, m,$$

where  $S_i^+$  is the distance between the  $i$ -th alternative and the positive ideal solution, and  $S_i^-$  is the distance between the  $i$ -th alternative and the negative ideal solution.

The evaluated values of the distance of each alternative from the positive-ideal (best) and the negative-ideal (worst) solutions are presented in Table 11.

**Table 11.** The values of the positive and negative separation distances.

Test no.	Positive separation distance	Negative separation distance
1	0.140	2.630
2	0.328	2.627
3	0.940	1.882
4	1.403	1.639
5	0.203	2.584
6	0.314	2.621
7	0.637	2.632
8	2.761	0.005
9	0.808	2.039
10	0.349	2.435
11	0.668	2.369
12	2.103	0.760

*Step 6.* Closeness coefficient of each alternative solution.

The relative closeness of each alternative to the positive ideal solution is calculated using Eq. (3.15):

$$(3.15) \quad C_i = \frac{S_i^-}{S_i^+ + s_i^-},$$

where  $0 < C_i \leq 1$ ,  $i = 1, 2, \dots, m$ .

*Step 7.* Ranking the preference order.

The ranking order is to be managed with respect to the values of closeness coefficient ( $C_i$ ) in descending order from 0 to 1. The value which is closest to 1 attains the first rank and it should be selected as the best among multiple decision-making response variables. The evaluated values for each alternative/experiment and corresponding ranking are presented in Table 12.

From the calculation and closeness coefficient presented in Table 11, it can be concluded that the value of closeness coefficient corresponding to experiment 11 with a drill speed and feed rate at 11 m/min and 0.05 mm/rev, respectively, is the optimal combination of process parameters to achieve minimal value for surface roughness, roundness error and feed force.

**Table 12.** The values of closeness coefficient and ranking.

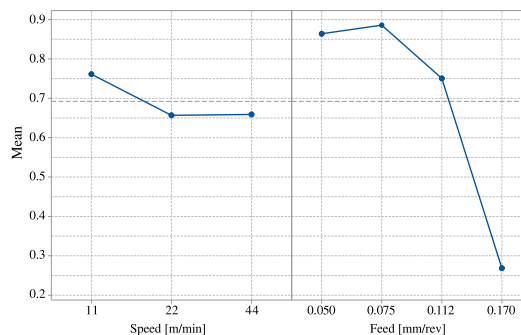
Test no.	Closeness coefficient	Ranking
1	0.950	1
2	0.889	4
3	0.667	9
4	0.539	10
5	0.927	2
6	0.893	3
7	0.805	6
8	0.002	12
9	0.716	8
10	0.875	5
11	0.780	7
12	0.265	11

### 3.4. ANOVA for closeness coefficient

ANOVA is a statistical method used to understand the effect of process parameters on multiple response characteristics. The analysis was performed at a 95% confidence interval, and the results of ANOVA for the closeness coefficient are presented in Table 13. The results of factor response are considered using the higher-the-better criteria and employing MINITAB software.

**Table 13.** ANOVA for weighted closeness coefficient.

Factors	DF	Seq SS	Adj MS	% Contribution	F-Value	P-Value
Speed [m/min]	1	0.01576	0.01576	1.68	0.54	0.480
Feed rate [mm/rev]	1	0.66089	0.66089	70.45	22.76	0.001
Error	9	0.26139	0.02904	27.87		
Total	11	0.93804				

**FIG. 8.** Main effect plot for weighted closeness coefficient.

ANOVA results reveal that the feed rate is most significant parameter, with a P-value of 0.001 ( $<0.05$ ) and a contribution of 70.45%, followed by a drill speed with a contribution of 1.68%.

As shown in Fig. 8, it is more significantly affected by feed rate rather than drill speed.

### 3.5. Confirmatory tests for TOPSIS

After the evaluation of optimal process parameter using TOPSIS, confirmatory tests were conducted two times with a drill speed of 11 m/min and a feed rate of 0.05 mm/rev. The results of confirmatory experiments are shown in Table 14.

**Table 14.** Results from the confirmatory experiment.

Sr. no.	Surface roughness [ $\mu\text{m}$ ]	Roundness error [ $\mu\text{m}$ ]	Feed force [N]
1	2.12	18.45	194.11
2	2.21	18.44	195.1
Average	2.17	18.45	194.61

The results of the confirmatory experiment were compared with the results of test no. 8 which had a minimal value of the closeness coefficient of 0.02 under the worst machining parameters. The comparative results are presented in Table 15. The closeness coefficient calculated for the confirmatory experiment is 0.953. As observed in Table 11, there is a significant improvement in all response characteristics. The surface roughness of the drilled hole shows a 61.41% improvement, the roundness error in the drilled hole shows an 81.4% improvement and there is a reduction of feed force value by 61.31% during drilling. The improvement in the weighted closeness coefficient for the weighted closeness coefficient of the worst machining conditions is about 97.90%.

**Table 15.** Comparison of confirmatory experiment results.

	Worst machining condition	Optimal reinforcement		Improvement [%]
		Predicted	Experimental	
Drill speed [m/min]	22	11	11	
Feed rate [mm/rev]	0.17	0.05	0.05	
Surface roughness [ $\mu\text{m}$ ]	5.62	2.2	2.17	61.41
Roundness error [ $\mu\text{m}$ ]	99.27	18.46	18.45	81.4
Feed force [N]	490.38	194.16	194.61	60.31
Weighted closeness coefficient	0.02	0.953		97.90

#### 4. CONCLUSIONS

Considering the current trend in the application of Al MMC in various engineering fields, it becomes necessary to determine the suitable machining parameters to improve the quality of machined specimen or work piece. The main aim of this work was to improve the quality of drilled hole in terms of minimizing surface roughness, reducing roundness error, and minimizing feed force during drilling operations. The results of this study involved selecting the best combination of drilling parameters from the range of parameters used in the experiment, guaranteeing the minimum surface roughness, the highest hole shape quality and the lowest feed force. The following conclusions have been made based on this work:

- It is evident that when we consider individual response we obtain different combinations of drilling parameters required to minimize each response and at the same time showing negative effect on another response.
- Drill speed has a significant effect on surface roughness and roundness error but it is not that much effective in the case of feed force. Changing the cutting speed results in a 65% difference in surface roughness and more than a threefold increase in roundness error. Maximum changes in feed force along with the change in drilling speed are at the level of 15%.
- Through EWTOPSIS, a drill speed of 11 m/min and a feed rate of 0.05 mm/rev are the best combination in the range of tested parameters to minimize surface roughness, roundness error, and feed force during the drilling of Saffil fiber-reinforced Al MMC.
- The results of this work can be used to improve the surface quality along with geometric accuracy and at the same time minimize feed force during drilling of Saffil fiber-reinforced Al MMCs.

#### REFERENCES

1. GILL R.S, SAMRA P.S., KUMAR A., Effect of different types of reinforcement on tribological properties of aluminium metal matrix composites (MMCs) – A review of recent studies, *Materials Today: Proceedings*, **56**(2): 3094–3101, 2022, doi: 10.1016/j.matpr.2021.12.211.
2. KUMAR A., GROVER N., MANNA A., CHOCHAN J.S., KUMAR R., SINGH S., PRUNCU C.I., Investigating the influence of WEDM process parameters in machining of hybrid aluminum composites, *Advanced Composite Letters*, **29**: 1–14, 2020, doi: 10.1177/2633366X20963137.
3. SINGH H., SINGH K., VARDHAN S., MOHAN S., A comprehensive review on the new developments consideration in a stir casting processing of aluminum matrix composites, *Materials Today: Proceedings*, **60**(2): 974–981 2022, doi: 10.1016/j.matpr.2021.12.359.
4. SIVASANKARAN S., HARISAGAR P.T., SAMINATHAN E., SIDDHARTH S., SASIKUMAR P., Effect of nose radius and graphite addition on turning of AA 7075-ZrB<sub>2</sub> in-situ composites, *Procedia Engineering*, **97**: 582–589, 2014, doi: 10.1016/j.proeng.2014.12.286.

5. KACZMAR J.W., NAPLOCHA K., MORGIEL J., Microstructure and strength of Al<sub>2</sub>O<sub>3</sub> and carbon fiber reinforced 2024 aluminum alloy composites, *Journal of Materials Engineering and Performance*, **23**(8): 2801–2808, 2014, doi: 10.1007/s11665-014-1036-2.
6. PUGAZHENTHI A., KANAGARAJ G., DINAHARAN I., RAJA SELVAM J.D., Turning characteristics of in situ formed TiB<sub>2</sub> ceramic particulate reinforced AA7075 aluminum matrix composites using polycrystalline diamond cutting tool, *Measurement*, **121**: 39–46, 2018, doi: 10.1016/j.measurement.2018.02.039.
7. NICHOLLS C.J., BOSWELL B., DAVIES I.J., ISLAM M.N., Review of machining metal matrix composites, *The International Journal of Advanced Manufacturing Technology*, **90**(9): 2429–2441, 2017, doi: 10.1007/s00170-016-9558-4.
8. KAROLCZAK P., KOŁODZIEJ M., KOWALSKI M., Effectiveness of diamond blades in the turning of aluminium composites, *Advances in Science and Technology Research Journal*, **14**(4): 262–272, 2020, doi: 10.12913/22998624/127436.
9. MARIMUTHU S., ANTAR M., DUNLEAVEY J., Characteristics of micro-hole formation during fibre laser drilling of aerospace superalloy, *Precision Engineering*, **55**: 339–348, 2019, doi: 10.1016/j.precisioneng.2018.10.002.
10. KUMAR H., CHOUDHARY R., SINGH S., Experimental and morphological investigations into electrical discharge surface grinding (EDSG) of 6061Al/ Al<sub>2</sub>O<sub>3p</sub> 10% composite by composite tool electrode, *Journal of Materials Engineering and Performance*, **23**(4): 1489–1497, 2014, doi: 10.1007/s11665-014-0899-6.
11. DESHMUKH S., JOSHI G., INGLE A., THAKUR D., An overview of aluminium matrix composites: particulate reinforcements, manufacturing, modelling and machining, *Materials Today: Proceedings*, **46**(17): 8410–8416, 2021, doi: 10.1016/j.matpr.2021.03.450.
12. HUANG S.T., ZHOU L., CHEN J., XU L.F., Drilling of SiCp/Al metal matrix composites with polycrystalline diamond (PCD) tools, *Materials and Manufacturing Processes*, **27**(10): 1090–1094, 2012, doi: 10.1080/10426914.2011.654152.
13. RAJMOHAN T., PALANIKUMAR K., KATHIRVEL M., Optimization of machining parameters in drilling hybrid aluminium metal matrix composites, *Transactions of Nonferrous Metals Society of China*, **22**(6): 1286–1297, 2021, doi: 10.1016/S1003-6326(11)61317-4.
14. TOSUN G., MURATOGLU M., The drilling of an Al/SiCp metal-matrix composites. Part I: Microstructure, *Composites Science and Technology*, **64**(2): 299–308, 2004, doi: 10.1016/S0266-3538(03)00290-2.
15. BUTOLA R., SHARMA V., KANWAR S., TYAGI L., SINGARI R.M., TYAGI M., Optimizing the machining variables in CNC turning of aluminium based hybrid metal matrix composites, *SN Applied Sciences*, **2**(8): 2020, doi: 10.1007/s42452-020-3155-8.
16. SENTHILKUMAR C., Optimisation of EDC parameters using TOPSIS approach, *International Journal of Machining and Machinability of Materials*, **21**(5/6): 480–492, 2019, doi: 10.1504/IJMMM.2019.103138.
17. RAMAKRISHNAN H., BALASUNDARAM R., SELVAGANAPATHY P., SANTHAKUMARI M., SIVASANKARAN P., VIGNESH P., Experimental investigation of turning Al 7075 using Al<sub>2</sub>O<sub>3</sub> nano-cutting fluid: ANOVA and TOPSIS approach, *SN Applied Sciences*, **1**(12): 1639, 2019, doi: 10.1007/s42452-019-1664-0.
18. REDDY P.V., RAMANJANEYULU P., REDDY B.V., RAO P.S., Simultaneous optimization of drilling responses using GRA on Al-6063/TiC composite, *SN Applied Sciences*, **2**(3): 431, 2020, doi: 10.1007/s42452-020-2214-5.

19. ABBAS C.A., HUANG C., WANG J., WANG Z., LIU H., ZHU H., Machinability investigations on high-speed drilling of aluminium reinforced with silicon carbide metal matrix composites, *The International Journal of Advanced Manufacturing Technology*, **108**: 1601–1611, 2020, doi: 10.1007/s00170-020-05409-4.
20. SHARMA V.S., DOGRA M., SURI N.M., Cooling techniques for improved productivity in turning, *International Journal of Machine Tools and Manufacture*, **49**(6): 435–453, 2009, doi: 10.1016/j.ijmactools.2008.12.010.
21. VARADARAJAN A.S., PHILIP P.K., RAMAMOORTHY B., Investigations on hard turning with minimal cutting fluid application (HTMF) and its comparison with dry and wet turning, *International Journal of Machine Tools and Manufacture*, **42**(2): 193–200, 2002, doi: 10.1016/S0890-6955(01)00119-5.
22. KANNAN C., VARUN CHAITANYA C.H., PADALA D., REDDY L., RAMANUJAM R., BALAN A.S.S., Machinability studies on aluminium matrix nanocomposite under the influence of MQL, *Materials Today: Proceedings*, **22**(4): 1507–1516, 2020, doi: 10.1016/j.matpr.2020.02.068.
23. XU J., JI M., CHEN M., REN F., Investigation of minimum quantity lubrication effects in drilling CFRP/Ti6Al4V stacks, *Materials and Manufacturing Processes*, **34**(12): 1401–1410, 2019, doi: 10.1080/10426914.2019.1661431.
24. CAROU D., RUBIO E.M., DAVIM J.P., A note on the use of the minimum quantity lubrication (MQL) system in turning, *Industrial Lubrication and Tribology*, **67**(3): 256–261, 2015, doi: 10.1108/ILT-07-2014-0070.
25. SZYMCZAK T., KOWALEWSKI Z.L., Brittle fracture of metal-ceramic composites [in Polish: Kruche pękanie kompozytów metalowo-ceramicznych], *Materiały kompozytowe*, **1**: 53–57, 2016.
26. AZO Materials, *Titanium (Ti) – Properties, Applications*, 2001, <https://www.azom.com/properties.aspx?ArticleID=1720>.
27. NAPLOCHA K., *Optimization of technological parameters in the manufacturing process of AK9 materials reinforced with Al<sub>2</sub>O<sub>3</sub> ceramic fibers* [in Polish], PhD Thesis, Wrocław University of Science and Technology, Wrocław, 1999.
28. SHANNON C.E., A mathematical theory of communication, *The Bell System Technical Journal*, **27**(3): 379–423, 1948, doi: 10.1002/j.1538-7305.1948.tb01338.x.
29. WANG E., ALP N., SHI J., WANG C., ZHANG X., CHEN H., Multi-criteria building energy performance benchmarking through variable clustering based compromise TOPSIS with objective entropy weighting, *Energy*, **125**: 197–210, 2017, doi: 10.1016/j.energy.2017.02.131.
30. MERT A., Shannon entropy-based approach for calculating values of WABL parameters, *Journal of Taibah University for Science*, **14**(1): 1100–1109, 2020, doi: 10.1080/16583655.2020.1804157.
31. DING X., CHONG X., BAO Z., XUE Y., ZHANG S., Fuzzy comprehensive assessment method based on the entropy weight method and its application in the water environmental safety evaluation of the Heshangshan drinking water source area, Three Gorges Reservoir Area, China, *Water*, **9**(5): 329, 2017, doi: 10.3390/w9050329.
32. KUMAR R., SINGH S., SINGH BILGA P., JATIN, SINGH J., SINGH S., SCUTARU M.L., PRUNCU C.I., Revealing the benefits of entropy weights method for multi-objective opti-

- mization in machining operations: A critical review, *Journal of Materials Research and Technology*, **10**: 1471–1492, 2021, doi: 10.1016/j.jmrt.2020.12.114.
33. HWANG C.L., YOON K., *Multiple Attribute Decision Making Methods and Applications: a State-of-the-Art Survey*, Springer: Berlin/Heidelberg, 1981.
  34. MANIVANNAN R., KUMAR M.P., Multi-attribute decision-making of cryogenically cooled micro-EDM drilling process parameters using TOPSIS method, *Materials and Manufacturing Processes*, **32**(2): 209–215, 2017, doi: 10.1080/10426914.2016.1176182.
  35. THIRUMALAI R., SENTHILKUMAAR J.S., Multi-criteria decision making in the selection of machining parameters for Inconel 718, *Journal of Mechanical Science and Technology*, **27**(4): 1109–1116, 2013, doi: 10.1007/s12206-013-0215-7.
  36. SINGH A., GHADAI R.K., KALITA K., CHATTERJEE P., PAMUČAR D., EDM process parameter optimization for efficient machining of Inconel-718, *FACTA UNIVERSITATIS Series: Mechanical. Engineering*, **18**(3): 473–490, 2020, doi: 10.22190/FUME200406035S.
  37. SINGARAVEL B., THANGIAH S., Application of integrated Taguchi and TOPSIS method for optimization of process parameters for dimensional accuracy in turning of EN25 steel, *Journal of the Chinese Institute of Engineers*, **40**(4): 267–274, 2017, doi: 10.1080/02533839.2017.1308233.
  38. YUVARAJ N., KUMAR M.P., Multi-response optimization of abrasive water jet cutting process parameters using TOPSIS approach, *Materials and Manufacturing Processes*, **30**(7): 882–889, 2015, doi: 10.1080/10426914.2014.994763.
  39. RABIEH M., RAFSANJANI A.F., BABAEI L., ESMAEILI M., Sustainable supplier selection and order allocation: an integrated Delphi method, fuzzy TOPSIS, and multi-objective programming model, *Scientia Iranica*, **26**(4): 2524–2540, 2019, doi: 10.24200/sci.2018.5254.1176.

*Received January 24, 2023; accepted version October 2, 2023.*



Copyright © 2023 The Author(s).

This is an open-access article distributed under the terms of the Creative Commons Attribution-ShareAlike 4.0 International (CC BY-SA 4.0 <https://creativecommons.org/licenses/by-sa/4.0/>) which permits use, distribution, and reproduction in any medium, provided that the article is properly cited. In any case of remix, adapt, or build upon the material, the modified material must be licensed under identical terms.